Journal of Innovative Optical Health Sciences
Vol. 5, No. 4 (2012) 1250028 (9 pages)

DOI: 10.1142/S1793545812500289

VISUALIZATION OF HEAD AND NECK CANCER MODELS WITH A TRIPLE FUSION REPORTER GENE

YING ZHENG[*,†], QIAOYA LIN[*,†,‡], HONGLIN JIN[*,†],
JUAN CHEN[‡] and ZHIHONG ZHANG[*,†,§]
[*]*Britton Chance Center for Biomedical Photonics*
Wuhan National Laboratory for Optoelectronics-Huazhong
University of Science and Technology, Wuhan 430074, P. R. China

[†]*MoE Key Laboratory for Biomedical Photonics*
Department of Biomedical Engineering
Huazhong University of Science and Technology
Wuhan 430074, P. R. China

[‡]*Campbell Family Cancer*
Research Institute and Ontario Cancer Institute
University Health Network, Toronto, P. R. Canada
[§]*czyzzh@mail.hust.edu.cn*

Accepted 10 August 2012
Published 5 October 2012

The development of experimental animal models for head and neck tumors generally rely on the bioluminescence imaging to achieve the dynamic monitoring of the tumor growth and metastasis due to the complicated anatomical structures. Since the bioluminescence imaging is largely affected by the intracellular luciferase expression level and external D-luciferin concentrations, its imaging accuracy requires further confirmation. Here, a new triple fusion reporter gene, which consists of a herpes simplex virus type 1 thymidine kinase (TK) gene for radioactive imaging, a far-red fluorescent protein (mLumin) gene for fluorescent imaging, and a firefly luciferase gene for bioluminescence imaging, was introduced for *in vivo* observation of the head and neck tumors through multi-modality imaging. Results show that fluorescence and bioluminescence signals from mLumin and luciferase, respectively, were clearly observed in tumor cells, and TK could activate suicide pathway of the cells in the presence of nucleotide analog-ganciclovir (GCV), demonstrating the effectiveness of individual functions of each gene. Moreover, subcutaneous and metastasis animal models for head and neck tumors using the fusion reporter gene-expressing cell lines were established, allowing multi-modality imaging *in vivo*. Together, the established tumor models of head and neck cancer based on the newly developed triple fusion reporter gene are ideal for monitoring tumor growth, assessing the drug therapeutic efficacy and verifying the effectiveness of new treatments.

Keywords: Head and neck cancer; tumor metastasis model; three fusion reporter gene; far-red fluorescent protein; firefly luciferase; multi-modality imaging.

1. Introduction

Head and neck cancers are one of the most dangerous malignant tumors that seriously affect the human health.[1–3] More than 52,000 cases are expected to be diagnosed and 7850 deaths are estimated.[4] in the United States in 2012 the five-year survival rate reach 61%.[5] Thus, great efforts must be paid to develop new probes and drugs and to improve therapeutic regimens for the diagnosis and treatment of head and neck cancers. Prior to these studies, effective *in vivo* tumor models are required to assist these attempts. Conventional models for head and neck cancers, such as the pharynx and oral cavity cancers, generally have difficulties in monitoring the tumor growth and metastasis due to their internal locations, which are invisible.[6] With the rapid progress in molecular imaging techniques, a number of reporter genes, most of which are fluorescent or luminescent, are used in small animal whole-body imaging and dynamic monitoring of tumor metastasis *in vivo*.[7–12] However, such reporter genes based imaging modalities[13] failed in providing an optimal balance between detection sensitivity and imaging depth *in vivo*.[14–16] Recently, a triple fusion reporter gene probe, which consists of a fluorescent protein reporter gene, a luciferase reporter gene and a herpes simplex virus type 1 thymidine kinase (TK) reporter gene, was created for multi-modality imaging, allowing high-brightness fluorescence imaging, low-background bioluminescence imaging and long-depth microPET imaging.[17–19]

In this work, we aimed to obtain a head and neck cancer cell line that stably expresses an improved triple fusion reporter gene, which was generated by replacing the fluorescent protein of the triple fusion reporter gene with a far-red fluorescent protein, mLumin, which is more suitable for *in vivo* imaging,[20–22] and to further establish head and neck cancer models based on this cell line. Taking advantages of the multi-modality imaging, and enhanced fluorescent signals and imaging depth through fluorescence imaging, these new tumor models will provide a valuable platform for real-time monitoring of the head and neck tumor growth and metastasis, as well as for therapeutic assessment (Fig. 1).

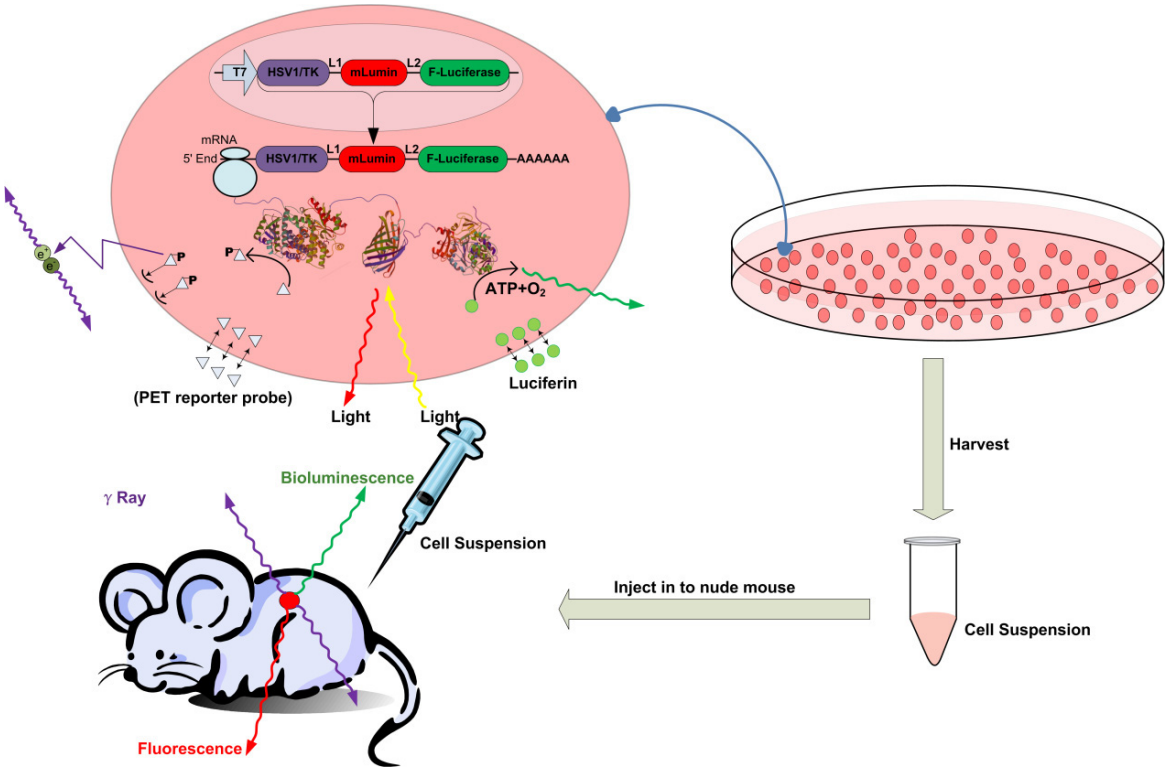

Fig. 1. Schematic diagram of the triple fusion reporter gene.

2. Materials and Methods

2.1. *Materials*

2.1.1. *Biomaterials*

The fluorescent protein gene TagRFP and mLumin were constructed in our laboratory previously. The firefly luciferase gene was provided as a gift by Dr Pritha Ray and Sanjiv Sam Gambhir in Clark Center, School of Medicine, Stanford University. The TK gene was acquired from Ariane Söling in the Molecular Neuro-oncology Laboratory, Department of Neurosurgery, Martin Luther University Halle-Wittenberg, D-06097 Halle, Germany. The cancer cell line KB was purchased from ATCC and 5-8F was donated by Dr Musheng Zeng in the Sun Yat-sen University Cancer Center of China.

2.1.2. *Apparatus*

PCR Thermal cycle instrument (Bio-Rad Laboratories Inc., California, USA), electrophoresis apparatus (Beijing LIUYI Inc., Beijing, China), CO_2 incubator (Thermo Scientific Inc., Massachusetts, USA), fluorescent inverted microscope IX-70 (OLYMPUS Co., Tokyo, Japan), GENios plus microplate reader (Tecan Group Ltd., Männedorf, Switzerland), FV1000 laser confocal microscope (OLYMPUS Co., Tokyo, Japan), IVIS Imaging System 100 (Caliperls Co., Massachusetts, US).

2.1.3. *Reagents*

RPMI 1640 culture medium, G418 and Lipofectamine ®2000 were purchased from Gibco-Invitrogen Co. (New York, USA), fetal bovine serum was obtained from Hyclone Co. (Utah, USA), MTT was obtained from Amresco Co. (Ohio, USA), Dual-Luciferase ® Reporter Assay System was purchased from Promega Co. (Wisconsin, USA) and D-Luciferin was obtained from Caliperls Co. (Massachusetts, USA)

2.2. *Methods*

2.2.1. *Plasmid construction*

To improve the fluorescent property of the triple fusion gene, we replaced the EGFP with mLumin and TagRFP [Figs. 2(b) and 2(c)], and obtained two triple fusion reporter genes, pcDNA3.1 (+)-TK-mLumin-Fluc and pcDNA3.1(+)-TK-TagRFP-Fluc, respectively. The plasmid of pcDNA3.1 (+)-Fluc was double digested by Hind III and EcoR I at the downstream of CMV promoter, annealed and linked to the primer S1:5′-AGCTTGGTACCGAGCTC GGTCCACTAGTCCAGTGTGGTGG-3′ and S2: 5′-AATTCCACCACACTGGACTAGTGGACC GAGCTCGGTACCA-3′. BamH I restriction enzyme sites were removed from the multiple cloning sites. The TK-EGFP gene was enzymatically digested and inserted to pcDNA3.1(+)-Fluc (No BamH I), and resulted in intermediate plasmid pcDNA3.1(+)-TK-EGFP-Fluc (EGFP with TAA). Subsequently, the target gene was amplified by PCR with mLumin as the template using the primer mLumin-F:5′-GGCTTAAGCTTGGTACC-GAGCTCGGATCCACCGGTCGCCACCA-TGGTGTCTAAGGGC-3′ and the mLumin-R:5′-C C G T T T A A A C G G G C C C T C T A G A CTCGAGGCTTCCGCCACTGCCACCATT-AAGTTTGTGC-3′. The EGFP gene in pcDNA3.1

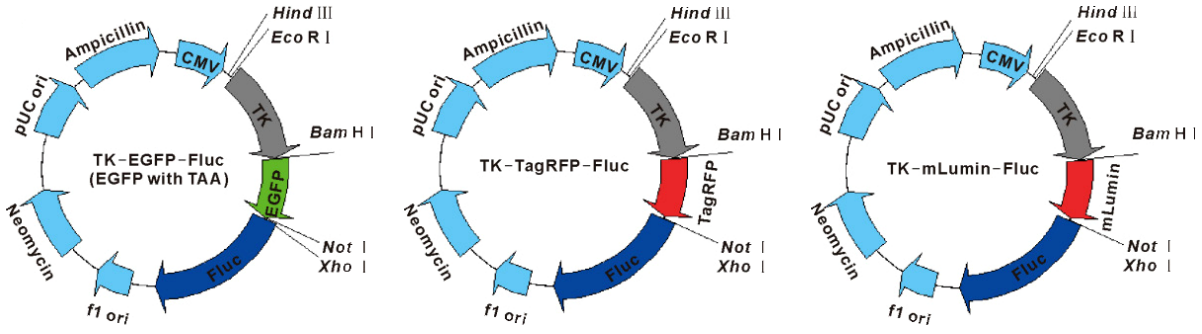

(a) (b) (c)

Fig. 2. Plasmid maps of the three fusion reporter genes including (a) pcDNA3.1(+)-TK-EGFP-Fluc with a stop code between EGFP and firefly luciferase gene, (b) pcDNA3.1(+)-TK-TagRFP-Fluc, and (c) pcDNA3.1(+)-TK-TagRFP-Fluc.

(+)-TK-EGFP-Fluc (EGFP with TAA) was replaced by the target gene after enzyme digestion and enzyme ligation, producing the final plasmid of the three fusion gene pcDNA3.1(+)-TK-mLumin-Fluc. The plasmid pcDNA3.1(+)-TK-TagRFP-Fluc was constructed using similar method. All the target fragment sequences were identical to the sequencing results.

2.2.2. *Identification of fluc activity in the plasmid*

All the cells were cultured at 37°C in a humidified 5% CO_2 incubator. A total of 1×10^4 5-8F cells were first seeded onto 96-well plates. Cells were transiently transfected with 100 ng pcDNA3.1 (+)-TK-mLumin-Fluc. 24 h later, fluorescence imaging was conducted using an inverted microscope (IX70) with an excitation filter (545−580 nm) and emission filter (610 LP). After the imaging, 20 μl lysate of the Dual-Luciferase ® Reporter Assay (promega) was added to the transfected 5-8F cells and original 5-8F cells (as a control) followed by the addition of 100 μl LARII of the Dual-Luciferase ® Reporter Assay (promega). About 5 min later, the bioluminescence was detected with a microplate reader.

2.2.3. *Identification of the TK activity via MTT assay*

The control group and the cells transfected with pcDNA3.1(+)-TK-mLumin-Fluc were exposed to 125 μg/ml ganciclovir (GCV) for 90 h. The medium was replaced by 100 μl RPMI 1640 supplemented with 10% FBS and 20 μl 5 mg/ml MTT was added to each well. After 4 h incubation, the medium was replaced by 100 μl DMSO. After the formazan was completely dissolved in DMSO, a microplate reader was employed to detect the absorption at 490 nm with a reference at 620 nm.

2.2.4. *Screening of the cell line stably expressing three fusion reporter protein*

KB cells were transfected with pcDNA3.1(+)-TK-mLumin-Fluc and pcDNA3.1(+)-TK-TagRFP-Fluc, respectively, followed by the screening using 1000 μg/ml G418 for four weeks. Then, cells expressed the red fluorescent protein was observed by the microscope.

2.2.5. *Confocal imaging*

About 2×10^4 KB-TK-mLumin-Fluc and KB-TK-TagRFP-Fluc cells were seeded onto the confocal petri dishes. Twenty-four hours later, confocal imaging was carried out under the following conditions: (1) 60X oil lens; (2) 543 nm laser; (3) PMT voltage: 730 V; (4) Excitation DM: DM 405/488/543; (5) Emission wavelength: 570−670 nm.

2.2.6. *Bioluminescence imaging*

About 1×10^5 KB-TK-mLumin-Fluc, KB-TK-TagRFP-Fluc and KB cells were seeded onto six-well plates, respectively, and cultured for 24 h. Prior to imaging, 8 μg/μl D-luciferin solution was prepared by dissolving 4 mg D-luciferin in 500 μl of 0.9% NaCl solution. Subsequently, 40 μl and 80 μl D-luciferin solutions were added to each cell line in 1 ml complete medium. The bioluminescence imaging was performed within 15 min using an IVIS Imaging System 100.

2.2.7. *Establishment of the KB-TK-mLumin-Fluc subcutaneous tumor model*

All animal studies were complied with the Hubei Provincial Animal Care and Use Committee and the Animal Experiment Guidelines of the Animal Experimentation Ethics Committee of Huazhong University of Science and Technology. Athymic Nude Mice (6−8 weeks) were subcutaneously injected into the root of the right lower leg with 2×10^6 KB-TK-mLumin-Fluc cells in 100 μl PBS. After the tumor diameter reached 0.5 cm, mice were intraperitoneally injected with 120 μl freshly prepared 10 mg/ml D-luciferin dissolved in 0.9% NaCl solution. Ten minutes later, mice were imaged by the Xenogen IVIS Imaging System 100 for bioluminescence measurement. For fluorescence imaging, the excitation and emission wavelength were set as 570 nm and 660 nm, respectively.

2.2.8. *Establishment of the KB-TK-mLumin-Fluc tail vein metastasis model*

Athymic nude mice (6−8 weeks) were intravenously injected with 2×10^6 KB-TK-mLumin-Fluc in 300 μl PBS. Cells were filtrated by a 20 μm filter to

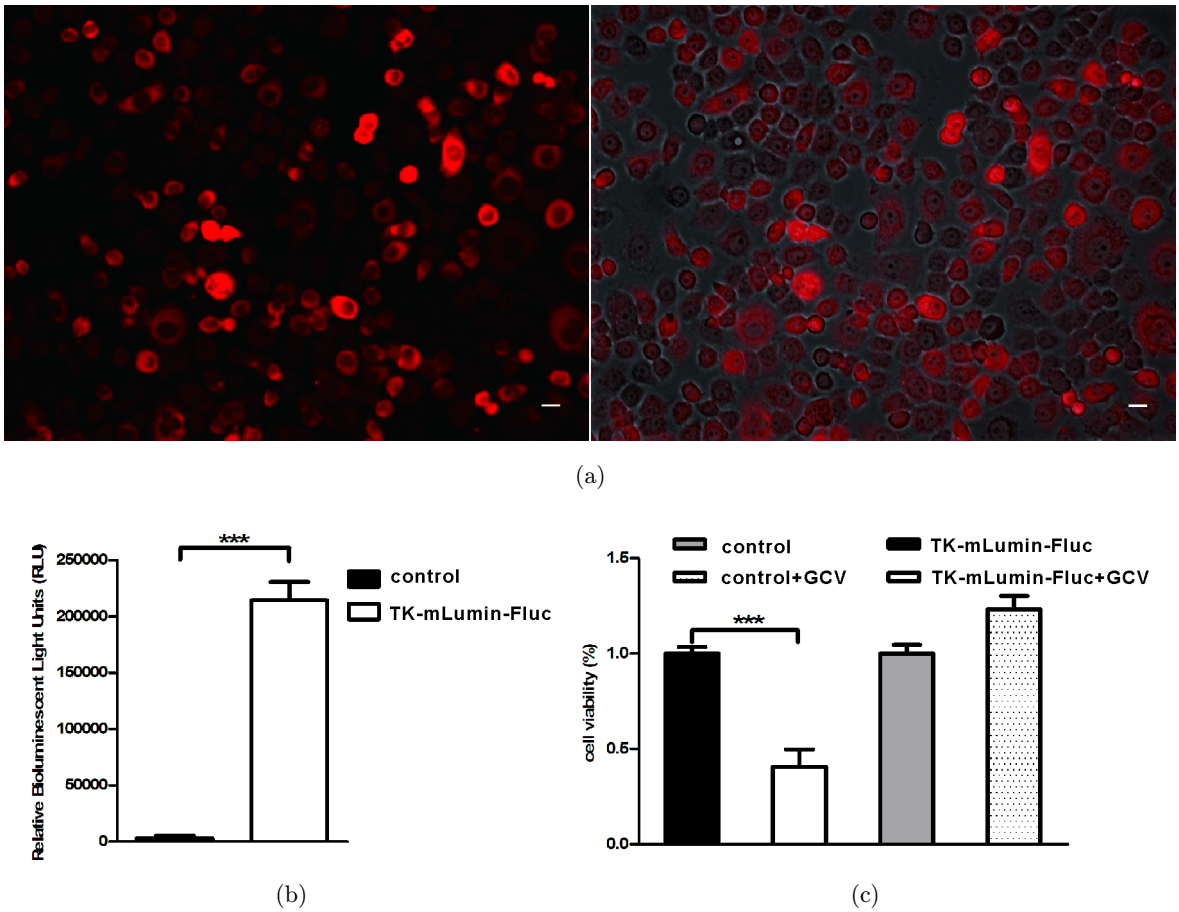

Fig. 3. The function validation of each reporter gene in plasmid. (a) The fluorescent imaging and the merge imaging of fluorescence and bright field channel, (b) the bioluminescent signal, and (c) the suicide activity of TK gene in 5-8F transiently transfected with pcDNA3.1(+)-TK-mLumin-Fluc. Scale bar, 20 μm. ***, $p < 0.001$.

remove large cell aggregates. Bioluminescence imaging was performed approximately four weeks post-injection using the same imaging conditions described above.

3. Results

3.1. *Biological activities of the improved triple fusion gene expressed by the cells*

In order to evaluate whether each gene still maintains the corresponding activity, the TK-mLumin-Fluc plasmid was transiently transfected to the cells as a proof of concept, and its fluorescence, bioluminescence and suicide activity, were tested using an inverted fluorescent microscope, a microplate reader and the MTT assay, respectively. As shown in Fig. 3(a), the fluorescence signal of mLumin was clearly observed at the red channel, indicating that the mLumin gene was functionally constructed into the triple fusion gene. After the cells were treated with D-luciferin for 5 min, results from the microplate reader show that the bioluminescence intensity of the cells transfected with TK-mLumin-Fluc was significantly higher than that of the control cells without the triple fusion gene, proving the effectiveness of the firefly Luciferase gene [Fig. 3(b)]. Moreover, the MTT result shows that the GCV significantly inhibited the growth of the cells transfected with TK-mLumin-Fluc. In contrast, the cell growth in control group was not significantly affected by GCV. Thus, the replacement of EGFP with far-red fluorescent proteins, such as mLumin, had no effect on the biological activities of the triple fusion gene.

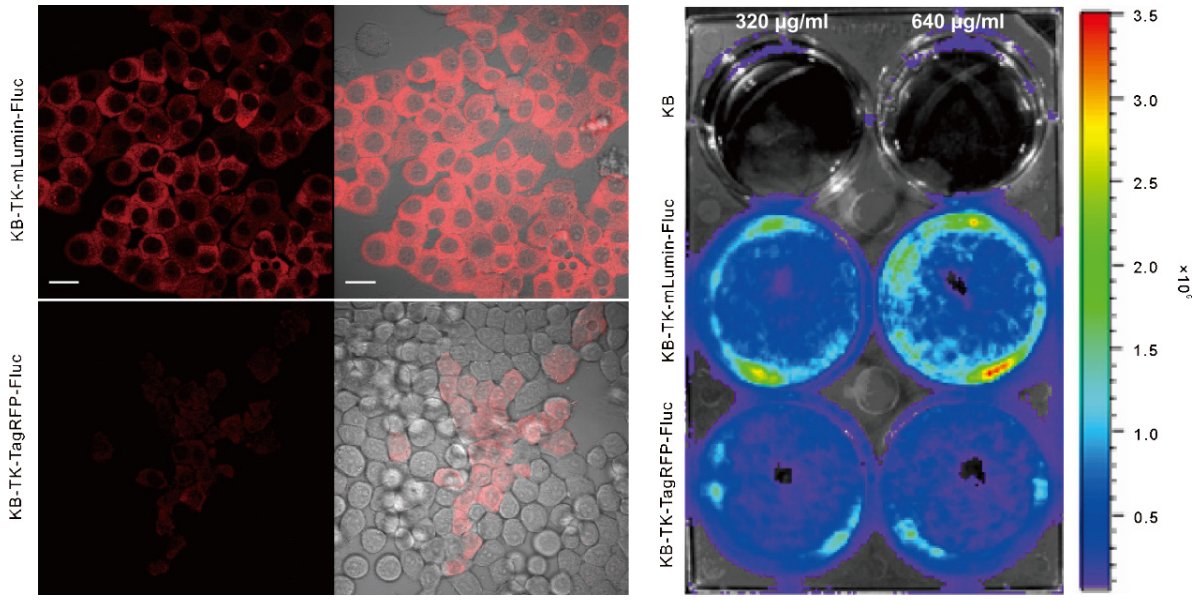

(a) (b)

Fig. 4. (a) Confocal imaging of KB-TK-mLumin-Fluc (top) and partially TK-TagRFP-Fluc expressing KB cell (down). Scale bar is 20 μm. (b) Bioluminescence imaging of KB, KB-TK-mLumin-Fluc and KB-TK-TagRFP-Fluc. The amount of D-luciferin added in the left vertical wells (320 μg/ml) is half of the right vertical wells (640 μg/ml).

3.2. *Preparation and characterization of the triple fusion gene-expressing cells*

After confirming that the triple report gene maintained its original functions, we obtained two cell lines with different expression levels of the triple fusion gene, KB-TK-mLumin-Fluc (over 90%) and KB-TK-TagRFP-Fluc (∼10%), and their fluorescent and bioluminescent properties were compared. As shown in Fig. 4(a), the fluorescent signal in KB-TK-mLumin-Fluc cells was much brighter than that in KB-TK-TagRFP-Fluc cells, suggesting that mLumin is more suitable than TagRFP for fluorescence imaging under current imaging condition [Fig. 4(a)]. Moreover, these fluorescent signals were highly correlated with the bioluminescent signals [Fig. 4(b)], in which cells with strong fluorescent signals accompanied with bright bioluminescent signals. Additionally, in the KB-TK-mLumin-Fluc cells, treatment with high concentration of D-luciferin resulted in increased bioluminescent signal. However, high-dosage D-luciferin treatment did not produce increased bioluminescent signal for the KB-TK-TagRFP-Fluc cells, possibly due to their relatively low expression of luciferase, suggesting that the bioluminescent signal of the cells are largely dependent on the luciferase expression level and the external D-luciferin dosage. Thus, the KB-TK-mLumin-Fluc cell line was selected for further *in vivo* studies, and preliminary information regarding the D-luciferin dosage and luciferase level was obtained.

3.3. *Tumorigenicity of KB-TK-mLumin-Fluc* in vivo

The nude mice were subcutaneously inoculated with KB-TK-mLumin-Fluc followed by the formation of a small bulge that grew bigger gradually. As the tumor size reached a certain level, bioluminescence and whole-body fluorescence imaging were conducted. As shown in Fig. 5, there was significant bioluminescence signal in the roots of the right lower extremity, and it correlated with remarkable fluorescent signal at the root of the right leg, indicating that a subcutaneous tumor model was successfully established, and this model could be used for multi-modality imaging.

3.4. *Metastasis of KB-TK-mLumin-Fluc* in vivo

Since KB-TK-mLumin-Fluc cells have tumorigenic ability, we consequently examined its metastatic potential in mice. Thirty days after tail vein injection, bioluminescence imaging was performed. As

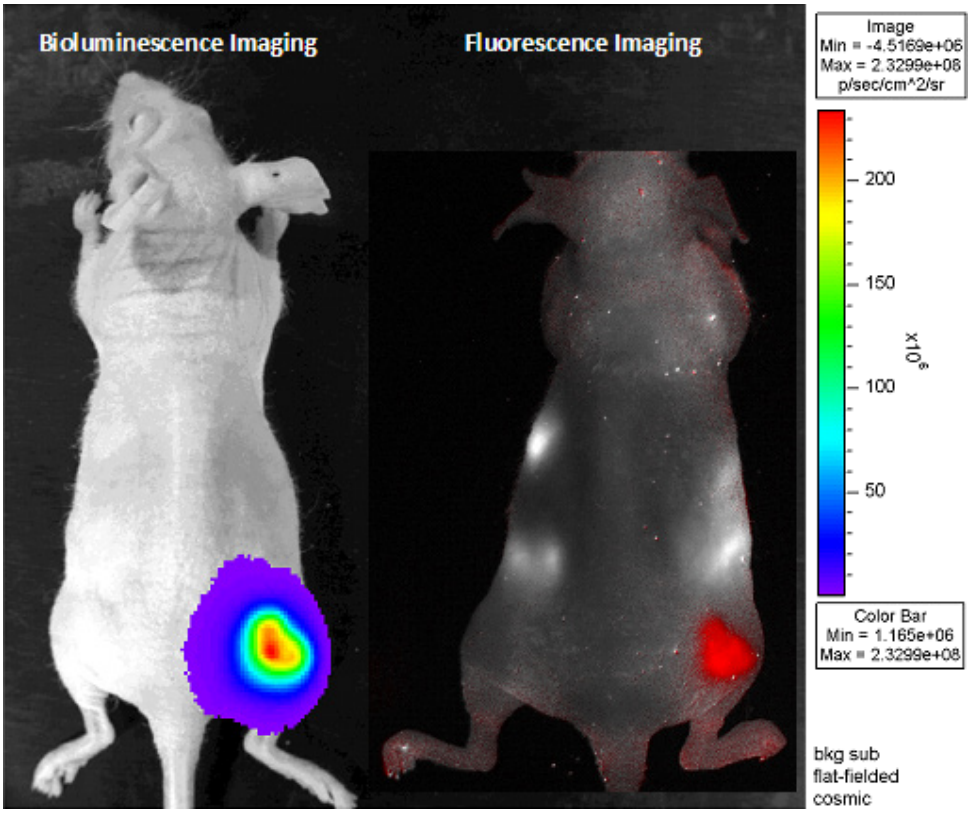

Fig. 5. Representative bioluminescent and fluorescent images of a nude mouse subcutaneously implanted with KB-TK-mLumin-Fluc cells.

shown in Fig. 6, bioluminescence signal was likely to have appeared at the right side of axillary lymph nodes and the left side of brachial lymph nodes in the nude mouse, suggesting that lymph node metastasis occurred in this animal model. Moreover, bioluminescence signal was also found at the lower abdomen of the mouse,[23] possibly in lumbar lymph nodes, sciatica lymph nodes or caudal lymph nodes. In addition, metastasis model for head and neck cancers based on triple fusion reporter gene could also be able to transfer to the brain and spinal (data not shown). Compared to the xenograft tumor model, this metastasis model showed no obvious fluorescent signal via the whole body fluorescent imaging (data not shown), which was likely due to the deep depth of the metastasis, and this might be further dealt with by microPET imaging systems.

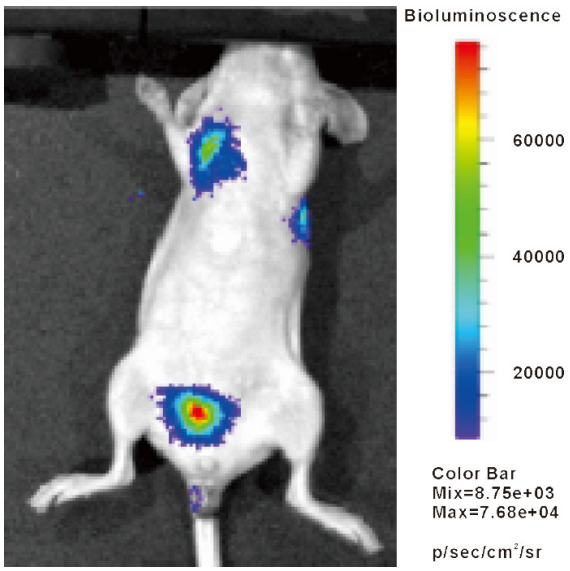

Fig. 6. Bioluminescent imaging of the KB-TK-mLumin-Fluc metastasis model.

4. Discussion

In this study, an improved triple fusion report gene was successfully constructed without losing its initial activities of fluorescence, bioluminescence and HSV1/TK. A head and neck cancer cell line stably expressing the plasmid (KB-TK-mLumin-Fluc) was further screened out and its corresponding subcutaneous tumor model and tail vein metastasis model

were established, respectively. Furthermore, effective detection of the tumor growth and metastasis was achieved via fluorescence imaging and bioluminescence imaging.

Previously established visible tumor models for head and neck cancer are generally based on EGFP or Luciferase.[24−30] However, their application was limited by the imaging depth of EGFP. Although bioluminescence based on luciferase is very sensitive and can accurately trace the tumor and metastasis location, it is unable to quantify the tumor size because the bioluminescence intensity partly depended on the D-Luciferase administration dosage.[31] Thus, we established an improved tumor model for head and neck cancer based on the triple fusion reporter gene. This model takes the advantages of intuitive, convenient and fast imaging of fluorescent protein (mLumin), low background of bioluminescence (Fluc) and long depth of microPET (TK) imaging. By combining the above three different imaging modalities, the real-time monitoring of tumor growth and metastasis in the animal models will be achievable.

In 2004, Gambhir group designed a triple fusion reporter gene, using TK, EGFP and Fluc, followed via an optimization with the replacement of EGFP by mRFP1.[19] In recent years, a variety of high-quality far-red fluorescent proteins have been identified and invented.[20,22,32] Among these, the use of far-red fluorescent proteins in the triple fusion reporter gene system would be expected to tremendously improve the quality of fluorescent imaging. Figure 3 proved that the improved triple fusion gene based on mLumin had the respective activities of fluorescent protein and luciferase. Additionally, TK gene could be further applied for PET imaging (Fig. 1). Basically, small nuclide molecules can be transferred into and out of cells freely through diffusion. In the presence of TK protein, the small nuclide molecules could be phosphorylated, preventing them from being flowing out of the cells. Moreover, TK, a thymus kinase derived from herpes simplex virus, can catalyze the phosphorylation of the nontoxic GCV into toxic compound (GCV-P), leading to the inhibition of DNA polymerase, early termination of DNA chain and thus generation of cytotoxicity against target tumor cells. Our results showed that GCV did inhibit the growth of cells transfected with the fusion reporter gene, indirectly proving the effectiveness of the TK reporter gene. Since the functional activity of the fusion protein may be declined due to the presence of steric hindrance between each functional block, further study is warranted to find the optimum linker between each protein.

The established KB-TK-mLumin-Fluc cell line provided a valuable cell model for multi-modality imaging at both *in vitro* and *in vivo* level. The subcutaneous tumor model of head and neck cancer based on the improved triple fusion reporter gene could be clearly observed by the luciferase reporter gene and the fluorescent protein reporter gene. Metastasis models that occurred in lymph nodes, brain and bone could be well tracked by bioluminescence imaging, and potentially via fluorescence molecular tomography (FMT) and PET imaging. Together, these new tumor models for head and neck cancer based on the improved triple fusion reporter gene can serve as important tools for the real-time monitoring of the occurrence and development of head and neck cancers, the assessment of the efficacy of new drugs, and the test of new therapeutic regimens.

Acknowledgments

We thank Dr Pritha Ray and Sanjiv Sam Gambhir for providing the firefly luciferase gene, Dr Ariane Söling for donating the TK gene and Prof Mu-Sheng Zeng for providing the 5-8F cell line. This work was supported by the National Science and Technology Support Program of China (Grant No. 2012BAI23B02), the China-Canada Joint Health Research Initiative (NSFC-30911120489, CIHR CCI-102936) and 111 Project of China (B07038). We thank the Analytical and Testing Center of Huazhong University of Science and Technology for spectral measurements.

References

1. A. A. Forastiere, A. Trotti, D. G. Pfister, J. R. Grandis, "Head and neck cancer: Recent advances and new standards of care," *J. Clin. Oncol.* **24**, 2603−2605 (2006).
2. M. Goerner, T. Y. Seiwert, H. Sudhoff, "Molecular targeted therapies in head and neck cancer — An update of recent developments," *Head Neck Oncol.* **2**, 8 (2010).
3. A. Jemal, R. Siegel, J. Xu, E. Ward, "Cancer statistics, 2010," *CA Cancer J. Clin.* **60**, 277−300 (2010).
4. "Head and Neck Cancer," National Cancer Institute at the National Institutes of Health, Available at http://www.cancer.gov/cancertopics/factsheet/Sites-Types/head-and-neck, 17 April (2012).

5. R. Siegel, D. Naishadham, A. Jemal, "Cancer statistics, 2012," *CA Cancer J. Clin.* **62**, 10−29 (2012).
6. D. Sano, J. N. Myers, "Xenograft models of head and neck cancers," *Head Neck Oncol.* **1**, 32 (2009).
7. P. Ray, A. De, "Reporter gene imaging in therapy and diagnosis," *Theranostics* **2**, 333−334 (2012).
8. P. Dubey, "Reporter gene imaging of immune responses to cancer: Progress and challenges," *Theranostics* **2**, 355−362 (2012).
9. I. Serganova, P. Mayer-Kukuck, R. Huang, R. Blasberg, "Molecular imaging: Reporter gene imaging," *Handbook Exp. Pharmacol.* **185** pt 2, 167−223 (2008).
10. J. H. Kang, J. K. Chung, "Molecular-genetic imaging based on reporter gene expression," *J. Nucl. Med.* **49**(2), 164S−179S (2008).
11. T. Imamura, A. Hanyu, A. Hikita, "*In vivo* optical imaging of cancer," *Seikagaku* **83**, 406−409 (2011).
12. K. O'Neill, S. K. Lyons, W. M. Gallagher, K. M. Curran, A. T. Byrne, "Bioluminescent imaging: A critical tool in pre-clinical oncology research," *J. Pathol.* **220**, 317−327 (2010).
13. T. F. Massoud, S. S. Gambhir, "Molecular imaging in living subjects: Seeing fundamental biological processes in a new light," *Genes Dev.* **17**, 545−580 (2003).
14. P. Mayer-Kuckuk, L. G. Menon, R. G. Blasberg, J. R. Bertino, D. Banerjee, "Role of reporter gene imaging in molecular and cellular biology," *Biol. Chem.* **385**, 353−361 (2004).
15. I. Serganova, R. Blasberg, "Reporter gene imaging: Potential impact on therapy," *Nucl. Med. Biol.* **32**, 763−780 (2005).
16. T. Boulin, J. F. Etchberger, O. Hobert, H. Hughes, "Reporter gene fusions," *WormBook*, ed. The C. elegans Research Community, pp. 1−23 (2006).
17. P. Ray, R. Tsien, S. S. Gambhir, "Construction and validation of improved triple fusion reporter gene vectors for molecular imaging of living subjects," *Cancer Res.* **67**, 3085−3093 (2007).
18. Y. J. Kim, P. Dubey, P. Ray, S. S. Gambhir, O. N. Witte, "Multimodality imaging of lymphocytic migration using lentiviral-based transduction of a trifusion reporter gene," *Molec. Imaging Biol.* **6**, 331−340 (2004).
19. P. Ray, A. De, J. J. Min, R. Y. Tsien, S. S. Gambhir, "Imaging tri-fusion multimodality reporter gene expression in living subjects," *Cancer Res.* **64**, 1323−1330 (2004).
20. D. Shcherbo, E. M. Merzlyak, T. V. Chepurnykh, A. F. Fradkov, G. V. Ermakova, E. A. Solovieva, K. A. Lukyanov, E. A. Bogdanova, A. G. Zaraisky, S. Lukyanov, D. M. Chudakov, "Bright far-red fluorescent protein for whole-body imaging," *Natl. Methods* **4**, 741−746 (2007).
21. J. Chu, Z. Zhang, Y. Zheng, J. Yang, L. Qin, J. Lu, Z. L. Huang, S. Zeng, Q. Luo, "A novel far-red bimolecular fluorescence complementation system that allows for efficient visualization of protein interactions under physiological conditions," *Biosens. Bioelectron.* **25**, 234−239 (2009).
22. X. Yang, H. Gong, J. Fu, G. Quan, C. Huang, Q. Luo, "Molecular imaging of small animals with fluorescent proteins: From projection to multimodality," *Comput. Med. Imaging Graph.* **36**, 259−263 (2012).
23. W. Van den Broeck, A. Derore, P. Simoens, "Anatomy and nomenclature of murine lymph nodes: Descriptive study and nomenclatory standardization in BALB/cAnNCrl mice," *J. Immunol. Methods* **312**, 12−19 (2006).
24. T. Liu, Y. Ding, W. Xie, Z. Li, X. Bai, X. Li, W. Fang, C. Ren, S. Wang, R. M. Hoffman, K. Yao, "An imageable metastatic treatment model of nasopharyngeal carcinoma," *Clin. Cancer Res.* **13**, 3960−3967 (2007).
25. J. D. Mocanu, E. H. Moriyama, M. C. Chia, J. H. Li, K. W. Yip, D. P. Huang, C. Bastianutto, B. C. Wilson, F. F. Liu, "Combined *in vivo* bioluminescence and fluorescence imaging for cancer gene therapy," *Molec. Imaging* **3**, 352−355 (2004).
26. S. Walenta, T. Schroeder, W. Mueller-Klieser, "Metabolic mapping with bioluminescence: Basic and clinical relevance," *Biomol. Engrg.* **18**, 249−262 (2002).
27. P. Tamulevicius, C. Streffer, "Metabolic imaging in tumours by means of bioluminescence," *Br. J. Cancer* **72**, 1102−1112 (1995).
28. D. M. Brizel, T. Schroeder, R. L. Scher, S. Walenta, R. W. Clough, M. W. Dewhirst, W. Mueller-Klieser, "Elevated tumor lactate concentrations predict for an increased risk of metastases in head-and-neck cancer," *Int. J. Radiat. Oncol. Biol. Phys.* **51**, 349−353 (2001).
29. J. H. Law, A. S. Whigham, P. S. Wirth, D. Liu, M. Q. Pham, S. Vadivelu, K. C. Kirkbride, B. T. Brown, B. B. Burkey, R. J. Sinard, J. L. Netterville, W. G. Yarbrough, "Human-in-mouse modeling of primary head and neck squamous cell carcinoma," *Laryngoscope* **119**, 2315−2323 (2009).
30. B. A. Neff, S. G. Voss, C. Allen, M. A. Schroeder, C. L. Driscoll, M. J. Link, E. Galanis, J. N. Sarkaria, "Bioluminescent imaging of intracranial vestibular schwannoma xenografts in NOD/SCID mice," *Otol. Neurotol.* **30**, 105−111 (2009).
31. T. Nakatsu, S. Ichiyama, J. Hiratake, A. Saldanha, N. Kobashi, K. Sakata, H. Kato, "Structural basis for the spectral difference in luciferase bioluminescence," *Nature* **440**, 372−376 (2006).
32. R. Dieguez-Hurtado, J. Martin, I. Martinez-Corral, M. D. Martinez, D. Megias, D. Olmeda, S. Ortega, "A Cre-reporter transgenic mouse expressing the far-red fluorescent protein Katushka," *Genesis* **49**, 36−45 (2011).